Electronic Supplementary Information (ESI)

Combining magnetic nanoparticle capture and poly-enzyme nanobead amplification for ultrasensitive detection and discrimination of DNA single nucleotide polymorphisms

Lorico D. S. Lapitan Jr.[a, b], Yihan Xu[a], Yuan Guo*[,c] and Dejian Zhou*[,a]

[a] School of Chemistry and Astbury Centre for Structural Molecular Biology, University of Leeds, Leeds LS2 9JT, United Kingdom.

[b] Department of Chemical Engineering, Faculty of Engineering, University of Santo Tomas, España Boulevard, Manila, Philippines.

[c] School of Food Science and Nutrition and Astbury Centre for Structural Molecular Biology, University of Leeds, Leeds LS2 9JT, United Kingdom.

* Corresponding authors.

Email: y.guo@leeds.ac.uk (Y. Guo) or d.zhou@leeds.ac.uk (D.Zhou)

S1. DNA Sequences and their abbreviations used in the study

Table S1. The name and sequences of DNA oligonucleotides used in this study.

DNA Name	DNA Sequence
Capture-DNA	PO_4^- - 5'- TGG CGT AGG CAA GAG TT_8 - 3' – DBCO *
Signal-DNA	Biotin- 5' - T_5 GTG GTA GTT GGA GCT G**G** - 3'
Wild type DNA (T1):	5'-ACT CTT GCC TAC GCC A**C**C AGC TCC AAC TAC CAC -3'
Cancer SNP 1 (T2)	5'-ACT CTT GCC TAC GCC A**T**C AGC TCC AAC TAC CAC -3'
Cancer SNP 2 (T3)	5'-ACT CTT GCC TAC GCC A**A**C AGC TCC AAC TAC CAC -3'

*DBCO = Dibenzocyclooctyne.

S2. Synthesis of NH_2-PEG_n-N_3 (n = ~23, MW =~1000) and PEG-PMAO amphiphilic polymer

The synthesis of amine-PEG_{23}-azide bifunctional linker was carried out in accordance to literature[1] with some modifications via the schematic diagram below.

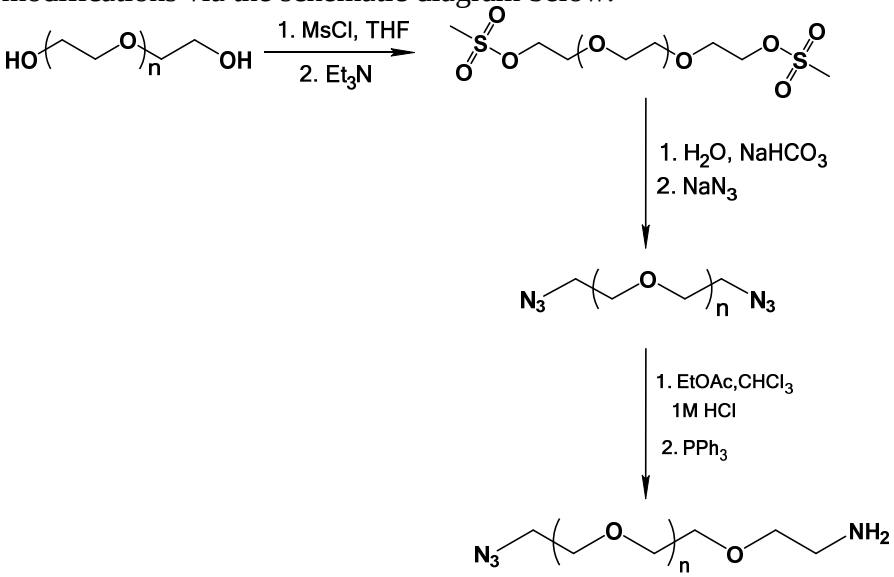

Scheme S1. The synthetic route to the NH_2-PEG_n-N_3 (n = ~23) bifunctional linker.

A) Synthesis of N_3-PEG_n-N_3 (n = ~23).

Poly(ethylene glycol) (MW =1000, 37.0 g, 37 mmol) was dissolved in 150 mL of dry THF containing methane sulfonylchloride (11.0 g, 92.5 mmol) in a 500 mL three neck round bottom flask equipped with an addition funnel, septa and magnetic stirrer. The mixture was stirred under N_2 atmosphere and cooled to 0 ºC in an ice bath. Triethylamine (13 mL, 92.5 mmol) was added dropwise to the mixture through the addition funnel over ~ 30 minutes. The reaction mixture was gradually warmed up to room temperature (20-25 ºC) and was left to stir for 12 hours. The mixture turned cloudy white and was filtered to remove the white powdery material. The product was checked by TLC with MeOH: $CHCl_3$= 1:15 (vol/vol) as elution solvent, R_f (MsO-PEG_{23}-OMs) = 0.14, R_f (OH-PEG_{23}-OH) = 0.08, R_f (N_3-PEG_{23}-N_3) = 0.20. The filtrate was transferred to a round bottom flask and diluted with water

[1] Susumu, Mei and Mattoussi, Multifunctional ligands based on dihydrolipoic acid and polyethylene glycol to promote biocompatibility of quantum dots. In *Nat. Protoc.*, 2009; Vol. 4, pp 424-436.

(150 mL) and added with $NaHCO_3$ (3.73 g, 44.4 mmol). The resulting mixture was transferred to a separation funnel and extracted with $CHCl_3$ (60 mL × 3). The combined organic phase was evaporated to dryness, yielding the desired product as a waxy solid (weight ~40 g).

The above product (40 g), sodium azide (10 g, 154 mmol), THF (50 mL), H_2O (50 mL) and $NaHCO_3$ (0.5 g) were added to a two-necked round bottom flask equipped with a distilling head connected to an ice bath cooled round bottom flask (as solvent trap). The reaction mixture was heated to distil off the THF. After complete removal of THF, the reaction mixture was refluxed overnight. The reaction mixture was cooled to room temperature and transferred to a separation funnel and then repeatedly extracted with $CHCl_3$ (100 mL × 5). The combined organic layers were dried over anhydrous Na_2SO_4 (~50 g, 30 min), filtered and then concentrated under vacuum to remove solvent, yielding a pale brown oil which solidified into a waxy material at low temperature (~ 53 g). A 1.50 g portion of the crude compound was purified by flash chromatography using silica gel with 15:1 (vol/vol) $CHCl_3$:MeOH as the eluent. Each fraction was checked by TLC (R_f for N_3-PEG-N_3 = 0.24) and the fractions containing the pure product were combined. After the solvent was removed, 0.852 g of the desired product (58% yield) was obtained. The chemical structure of the prepared N_3-PEG-N_3 was confirmed from its ^{1}H NMR spectra shown below.

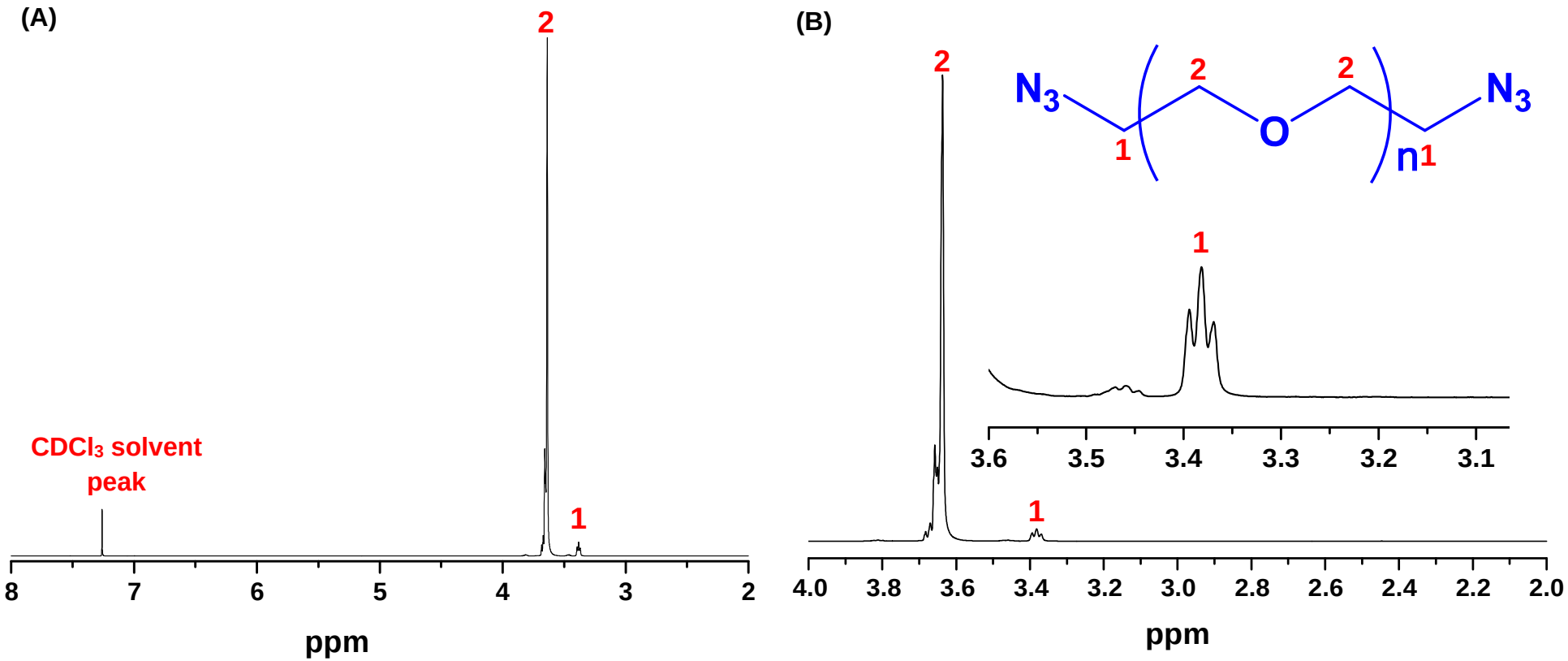

(**A**) ^{1}H NMR spectrum for N_3-PEG_{23}-N_3 (MW ~1000) in $CDCl_3$. (**B**) The enlarged regions showing proton assignment: the larger peaks at ~ 3.65 ppm are the CH_2 groups of the repeating PEG units. The 3.1 -3.6 ppm region was enlarged for clarity. The triplet peaks at ~3.4 ppm were the resonances of CH_2 groups of the terminal CH_2 connected to the azide group. ^{1}H NMR (400 MHz, $CDCl_3$ δ= 7.27 ppm): 3.65-3.70 (m), 3.35-3.4 (t, 4H, *J* = 5.0 Hz).

The chemical structure of N_3-PEG-N_3 linker was further characterized using mass spectrometry (Bruker maXis impact 2 spectrometer). The polyethylene glycol (average MW ~ 1000) used to synthesize the N_3-PEG-N_3 contained a mixture of different length ethylene glycol chains. The general molecular formula for the N_3-PEG-N_3 is $(CH_2)_2(C_2H_4O)_n N_6$:

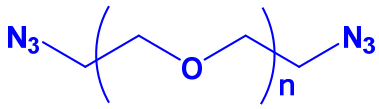

Where *n* is the number of the ethylene gylcol units (EG, MW = 44 g·mol^{-1}). The MW peaks reported in the mass spectra were determined to be the sodium ion adducts [MW + Na^+]. Therefore, the chain length of N_3-PEG-N_3 can be estimated from the formula: 135 + 144 *n*. The mass spectra of N_3-PEG-N_3 and the assignment of the corresponding EG chain length for each of the molecular ion peaks was shown below.

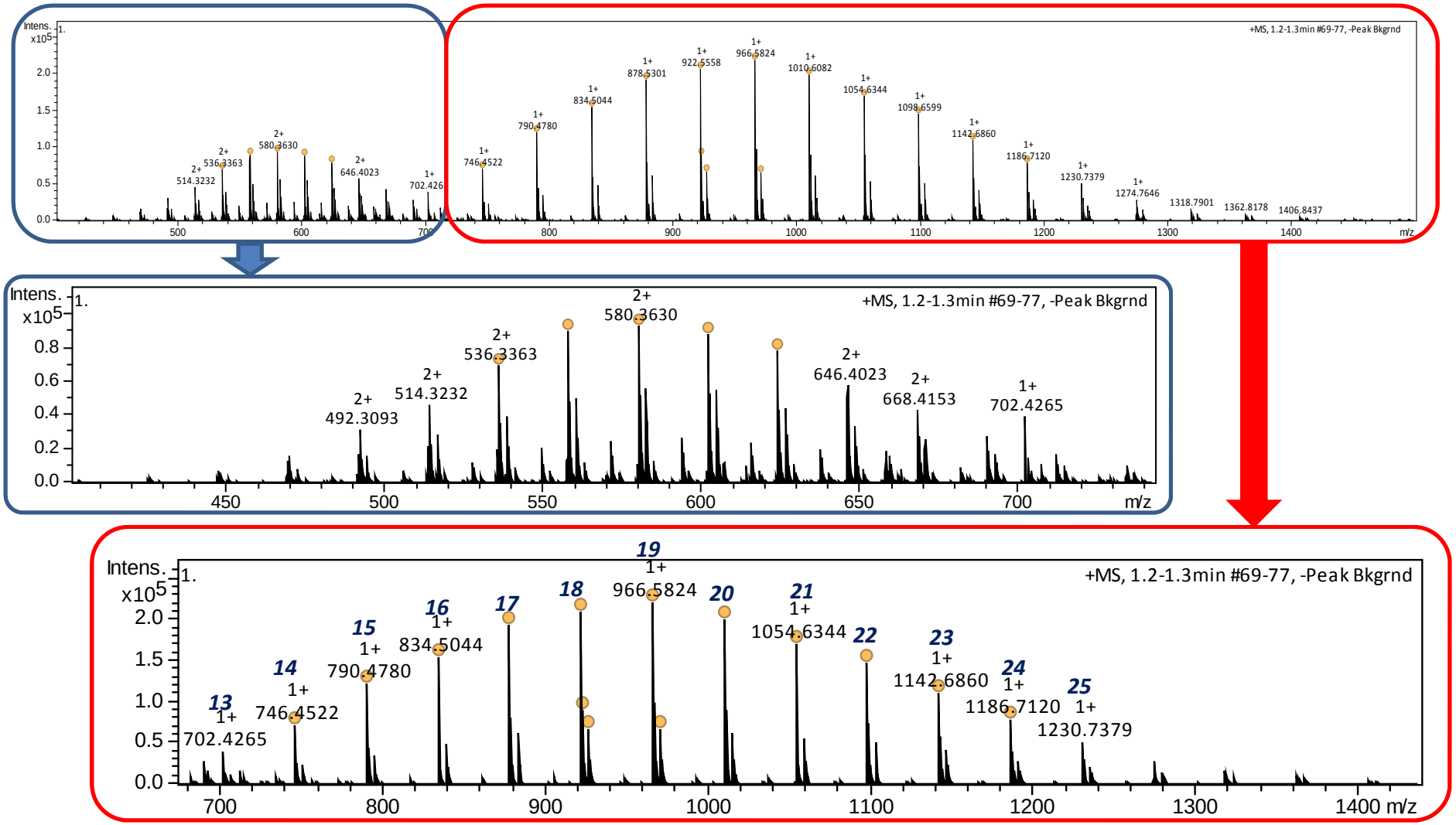

Typical mass spectra of N_3-PEG-N_3. The ion peaks are reported as **(**MW + Na^{1+}) and the corresponding ethylene glycol chain lengths were assigned to each molecular ion peak.

B) Amine transformation of one terminal azide group, N_3-PEG_n-NH_2 (n = ~23)

N_3-PEG-N_3 (4.5 g, 4.36 mmol) was dissolved in a mixture of 15 mL EtOAc and 15 mL $CHCl_3$ and 1.0 M HCl (10 mL, 10 mmol) in a 500 mL two necked round bottom flask equipped with an addition funnel, septa and magnetic stirrer. The solution was stirred under a N_2 atmosphere and cooled to 0ºC in an ice bath. Then triphenylphosphine (TPP, 1.25 g, 4.76 mmol) was dissolved in ethyl acetate (17.0 mL) and transferred to the addition funnel. The TPP solution was added dropwise to the reaction mixture while maintaining the temperature at 0-5ºC. After the addition was complete, the reaction was gradually warmed up to room temperature (20-25 ºC) and was stirred overnight (~12 hours) under a N_2 atmosphere. The biphasic mixture was transferred to a separation funnel and the aqueous layer was collected and washed EtOAc (100 mL × 2) to remove any unreacted TPP and triphenylphosphine oxide byproduct. The aqueous layer was transferred to a round bottom flask with a magnetic stirrer and placed in an ice bath. Potassium hydroxide (5.05 g, 90.0 mmol) was slowly added and the mixture was stirred until all solid KOH was dissolved. The aqueous layer was transferred to a clean separation funnel and was repeatedly extracted with EtOAc (100 mL × 5). The combined organic layers were dried over anhydrous Na_2SO_4 (~50 g, 30 min), filtered and concentrated under vacuum to yield a pale oil like product which solidified into a waxy material at low temperature (~5.1 g). A ~1.5 g portion of the crude compound was purified by column chromatography using silica gel with 5:1 (vol/vol) $CHCl_3$:MeOH as the eluent. Each fraction was checked by TLC (R_f for N_3-PEG-NH_2 = 0.28) and fractions containing the pure product were combined. After removal of the solvent, 0.875 g of the pure product was obtained (68% yield). The ^{1}H NMR spectra of the purified compound was shown below.

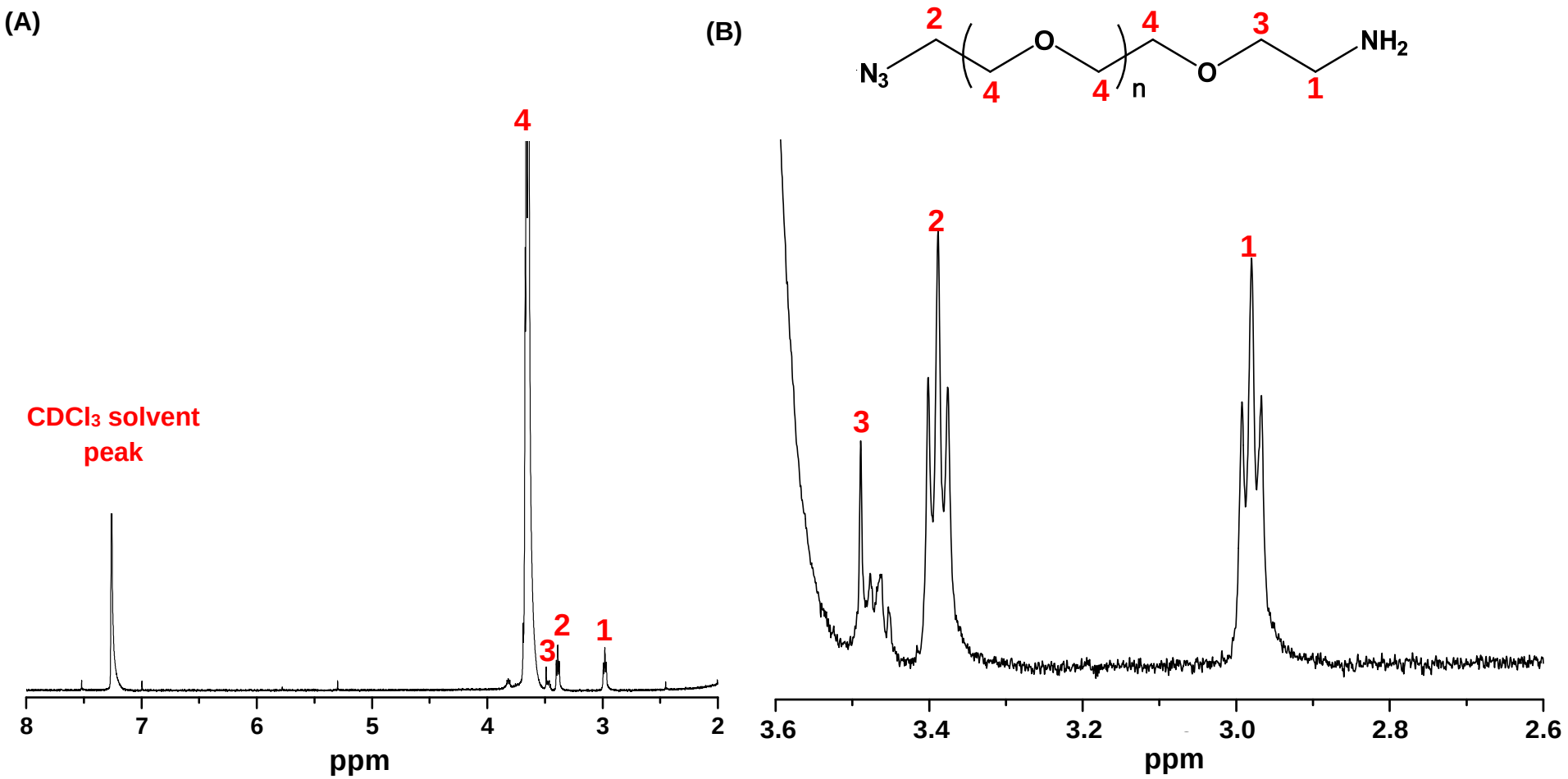

(**A**) ^{1}H NMR spectrum for NH_2-PEG_n-N_3 in $CDCl_3$ (average MW ~ 1000, n = ~23). (**B**) The enlarged 2.6 -3.6 ppm region showing proton assignment. The residual methanol peak is observed at ~ 3.48 ppm. ^{1}H NMR (400 MHz, δ ppm): 7.27 ($CDCl_3$ solvent peak); 3.65-3.70 (m, -C<u>H</u>$_2$ in PEG repeat units, **4**), 3.52 (m, -C<u>H</u>$_2$, **3**), 3.40 (t, 2H, *J* = 4.8 Hz, -C<u>H</u>$_2$-N_3, **2**), 2.89 (t, 2H, *J* = 5.0 Hz, -C<u>H</u>$_2$-NH_2, **1**).

The chemical structure of NH_2-PEG-N_3 was further characterized using mass spectrometry. The general molecular formula of the desired NH_2-PEG-N_3 product can be described as $(CH_2)_2(C_2H_4O)_nH_2N_4$:

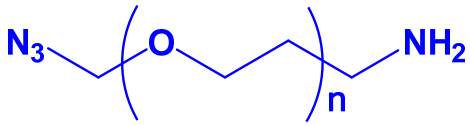

The MW peaks [MW+H^+] for the desired NH_2-PEG$_n$-N_3 product with different EG chain lengths were estimated from the formula (87 + 44 *n*). The mass spectra of NH_2-PEG-N_3 and the assignment of the corresponding EG chain length for each molecular ion peak were shown below.

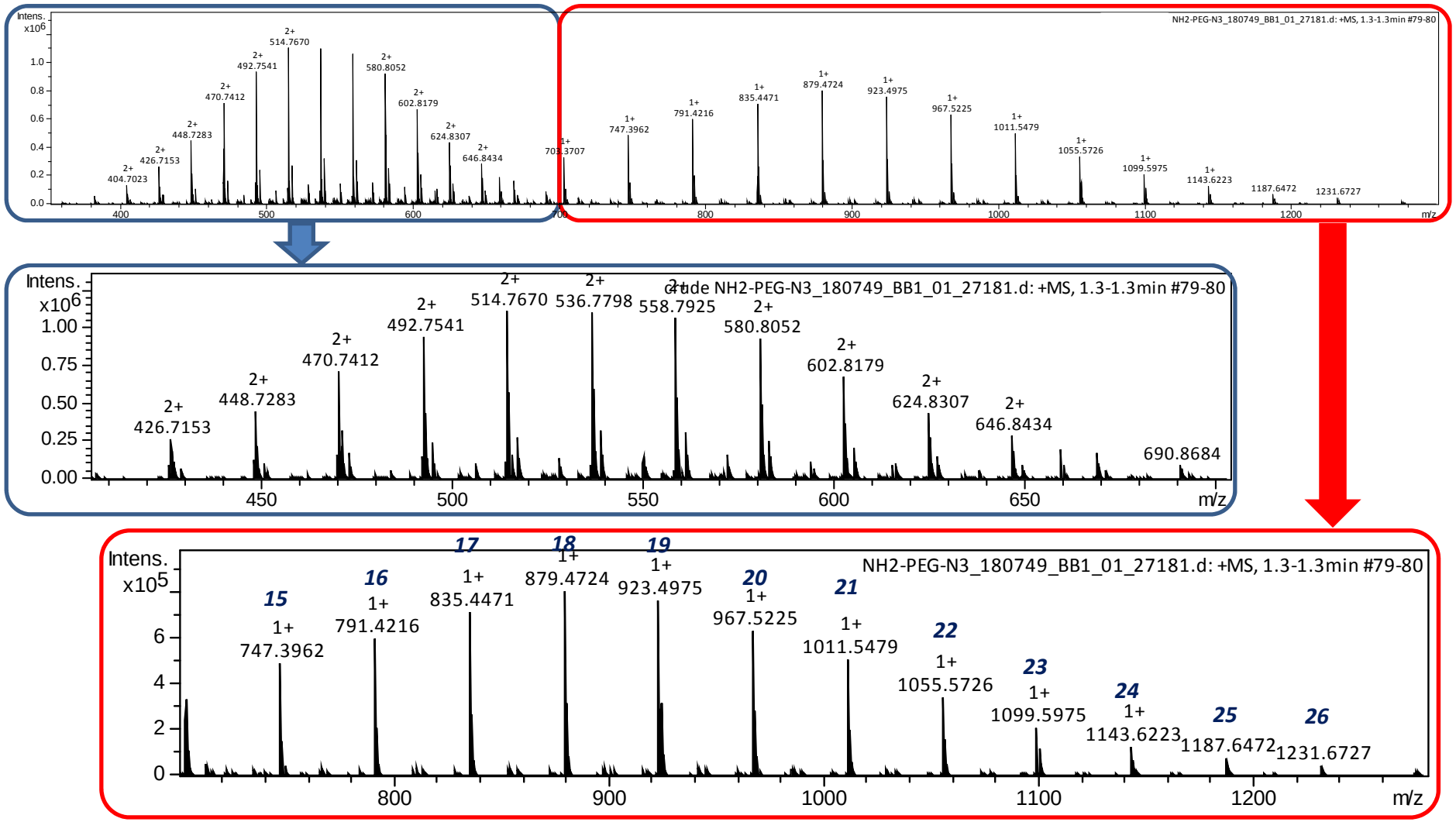

Mass spectra of NH_2-PEG-N_3. The ion peaks are reported as (MW+H^{1+}) and the corresponding ethylene glycol chain lengths were assigned to each molecular ion peak.

C). Preparation of amphiphilic PEG-PMAO copolymer

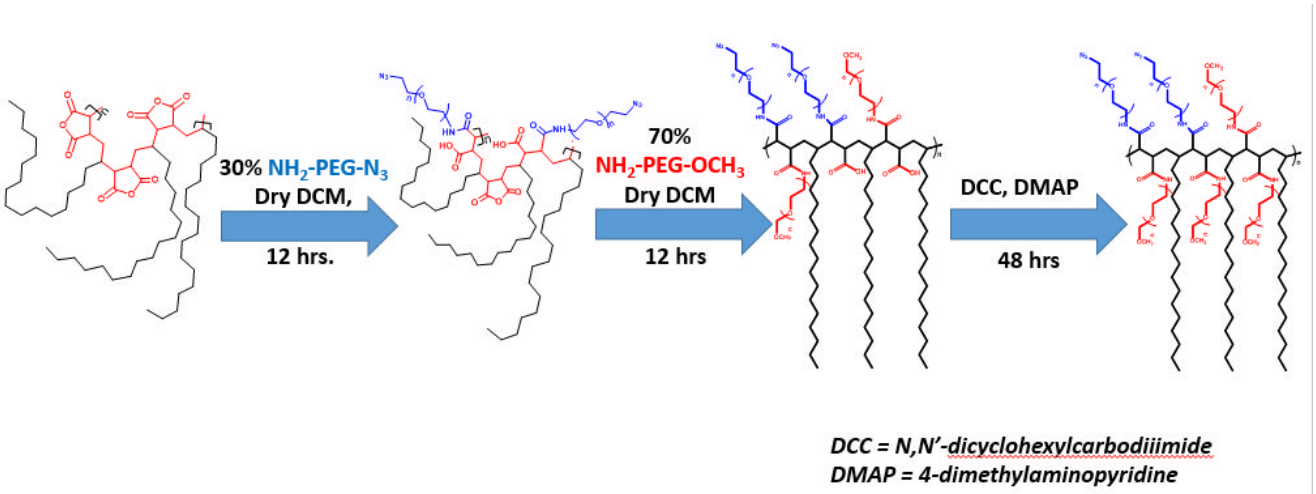

Scheme S2. Synthetic route to amino-PEG modified PMAO amphiphilic

The calculation below served as a guideline to determine the weights of the PEG linkers needed to graft to PMAO. The calculations were based on the reactive monomer unit of PMAO ($C_{24}H_{42}O_3$) with a MW of 378 g·mol^{-1}.

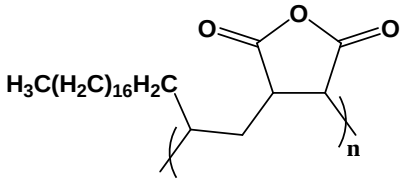

- Number of moles of PMAO unit in 0.250 g PMAO

$$\frac{0.250}{378} = 6.61 \times 10^{-4}\ mole$$

- Number of moles of PEG reagents needed (each PMAO unit can react with 2 equivalents of the NH_2-PEG reagent at 100% grafting density).

$$6.61 \times 10^{-4}\ mole \times 2 = 1.32 \times 10^{-3}\ mole$$

- Weight of NH_2-PEG_n-OCH_3 (n ~23) required (70% grafting density)

$$1.32 \times 10^{-3}\ mole \times 0.70 \times \frac{1000\ g}{mole} = 0.923\ g$$

- Weight of NH_2-PEG_n-N_3 (n ~23) required (30% grafting density)

$$1.32 \times 10^{-3}\ mole \times 0.30\ x\ \frac{1000\ g}{mole} = 0.396\ g$$

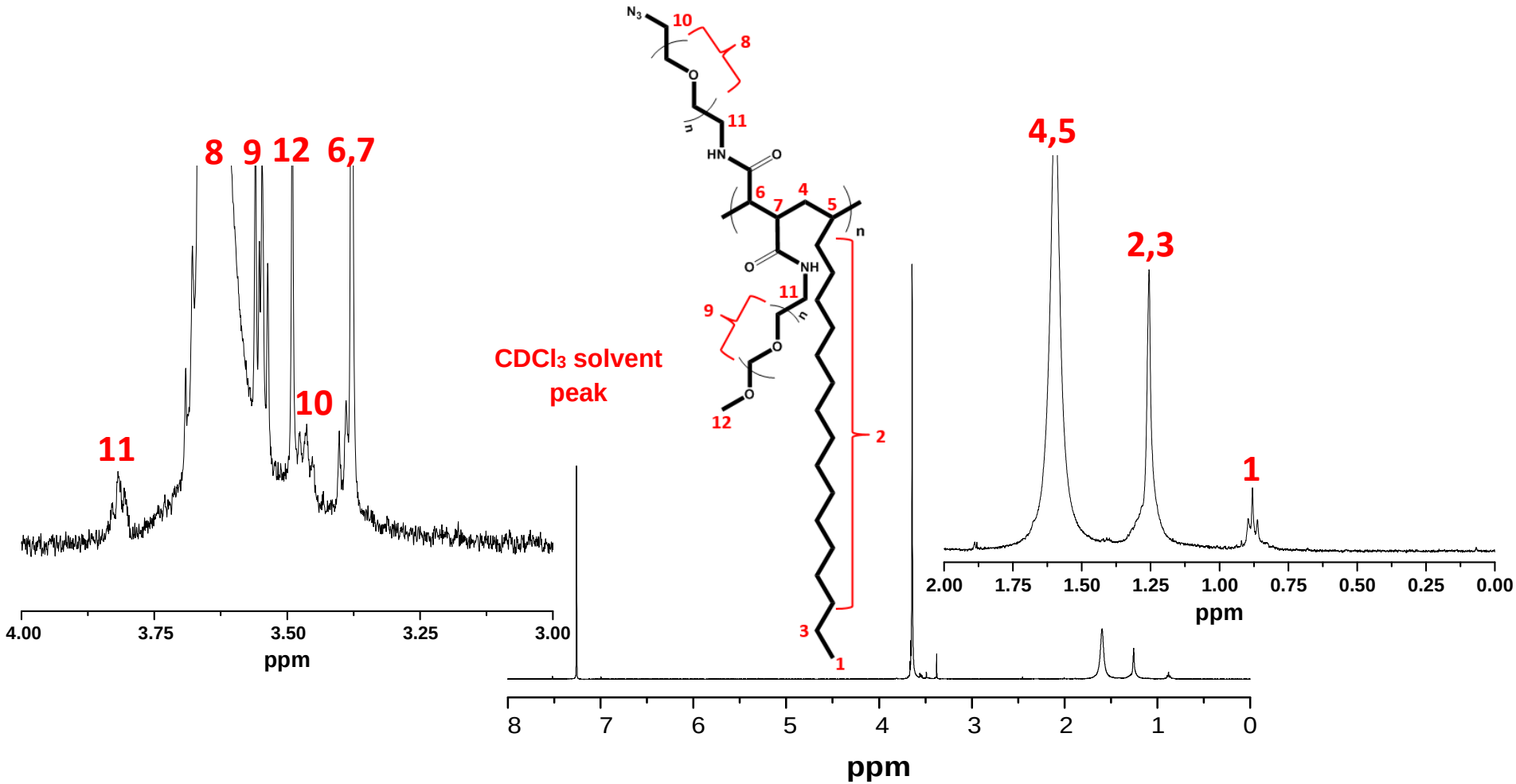

^{1}H-NMR spectra of the prepared PEG-PMAO polymer. The characteristic peaks of alkyl chains (C_{16}) in PMAO were observed at ~1.25 ppm. The peak of amide bond was weak due to low abundance as compared to the protons of the alkyl chain and the PMAO backbone. ^{1}H NMR (400 MHz, δ ppm); 0.80, -$(CH_2)_{15}C\underline{\mathbf{H}}_3$; 1.25, -$(C\underline{\mathbf{H}}_2)_{14}C\underline{\mathbf{H}}_2$-$CH_3$; 1.55-1.70, -C**H**-C**H**-; 3.38-3.42, C(O)-C**H**-C**H**-; 3.40, -$C\underline{\mathbf{H}}_2$-$N_3$; 3.50, -O-$C\underline{\mathbf{H}}_3$; 3.55-3.70, -$(C\underline{\mathbf{H}}_2$-O-$C\underline{\mathbf{H}}_2)_n$; 3.80, -NH-$C\underline{\mathbf{H}}_2$-; 7.37 ($CDCl_3$ solvent peak)

S3. Calculation of surface biotin on polymer beads using HABA assay

The calculation was based on the assay protocol provided by the supplier. The change in the absorbance at 500 nm for the HABA/Avidin complex upon addition of the sample was calculated as follows:

$$\Delta A_{500} = 0.9\left(Abs_{HABA/Avidin}\right) - \left(Abs_{HABA/Avidin\ +sample}\right)$$

Where 0.9 is the dilution factor of HABA/Avidin upon addition of sample.

The amount of biotin was calculated as:

$$\frac{\mu mole\ biotin}{mL} = \frac{\Delta A_{500}}{34}$$

The change in absorbance at 500 nm was divided by 34 $mM^{-1}\cdot cm^{-1}$ (the extinction coefficient of HABA/Avidin at 500 nm). The original biotinylated sample was diluted 10-fold in the reaction mixture. Therefore, a multiplier of 10 is used in this step to convert the biotin concentration in the reaction mixture to the biotin concentration in the original sample. Finally, the extent of biotin labelling can be computed as:

$$\frac{molarity\ of biotin}{molarity\ of\ polymer\ nanobead}$$

S4. Encapsulation and dispersion stability of polymer encapsulated MNPs

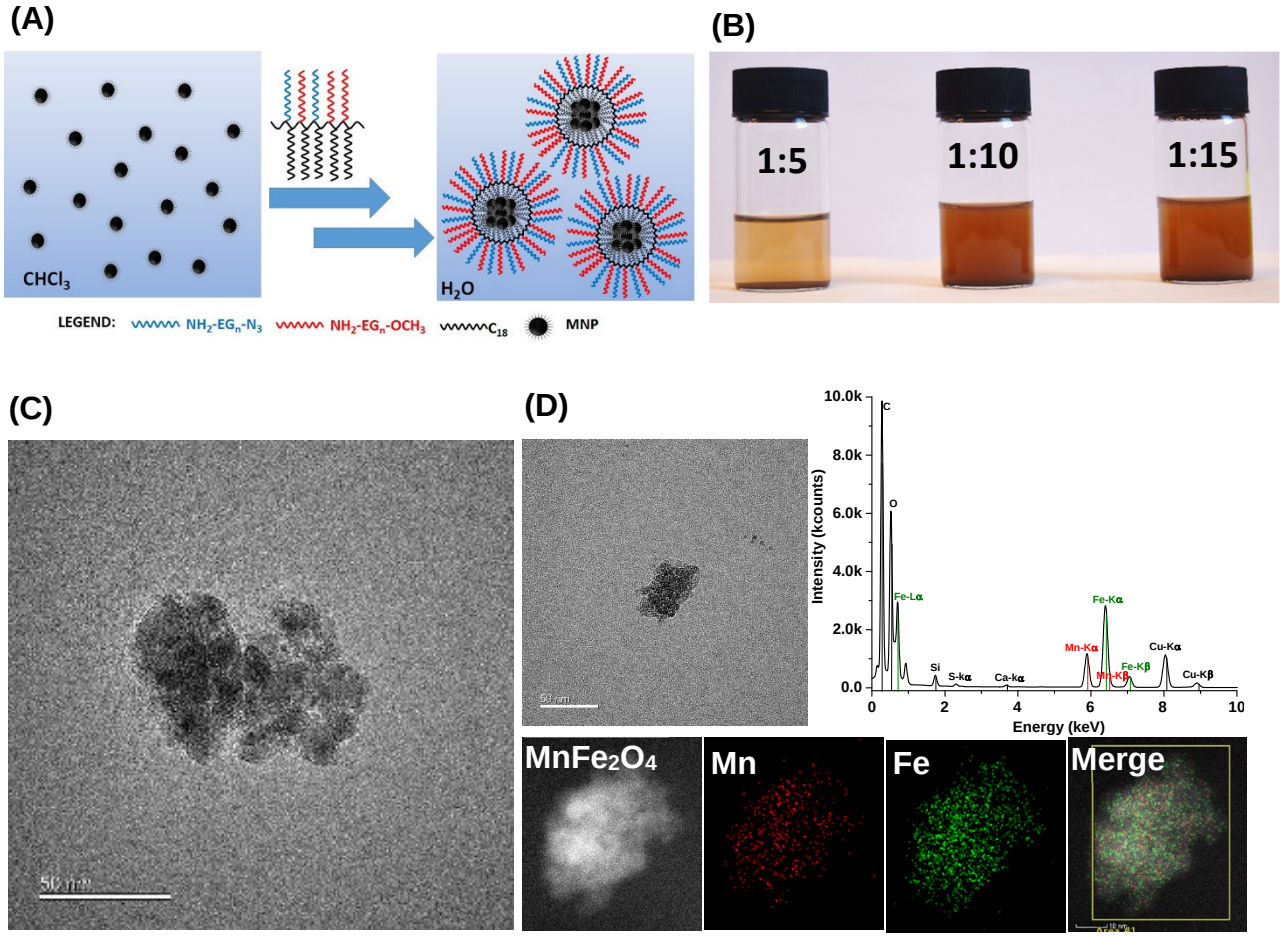

Figure S1. (**A**) Schematic diagram of polymer coating and stabilization of MNPs in aqueous solution. The amphiphilic PMAO-PEG encapsulates the hydrophobic MNPs via multiple hydrophobic-hydrophobic interactions between the polymer alkyl chains and the MNP surface hydrophobic ligands, leaving the hydrophilic PEG arms exposed to the aqueous environment to provide stable dispersion. (**B**) Photographs of polymer encapsulated MNPs dispersed in water under different polymer:MNP weight ratios after standing for 24 h. The 1:5 sample is mostly precipitated but the 1:10 and 1:15 samples still show good water-dispersability. (**C**) A TEM image of the polymer coated $MnFe_2O_4$ nanoparticles showing a clustered morphology of smaller MNPs with an overall magnetic core size of ~90 nm (scale bar 50 nm). (**D**) Energy Dispersive X-ray (EDX) spectrum of a MNP cluster (scale bar 50 nm) for elemental analysis showing the presence of Mn (red dots) and Fe (green dots) atoms. This was further confirmed by elemental mapping using high angle annular dark field (HAADF).

S5. Effect of capture DNA loading

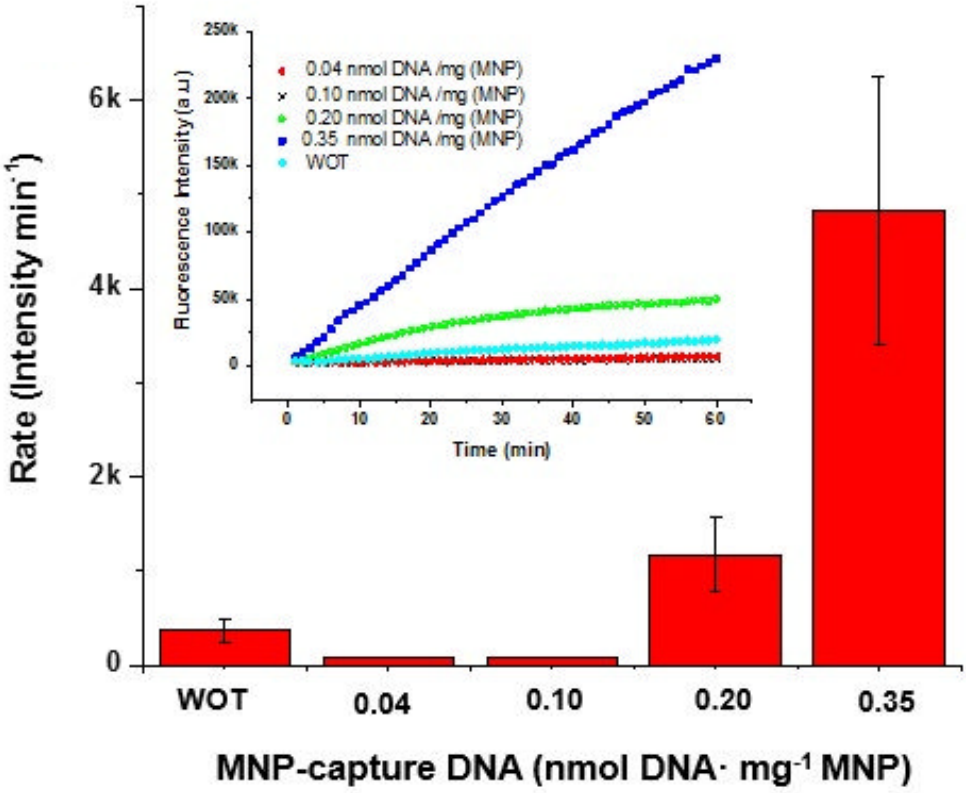

Figure S2. Comparison of fluorescence response (slopes of fluorescence response curves shown in figure inset) for MNP-DNA conjugates with different capture DNA loadings (*n* =3). Figure inset: typical time-dependent fluorescence intensity profiles for detecting perfect match T1 for MNP-capture DNA with different capture DNA loading.

S6. DNA Biosensing using single NAV-HRP amplification

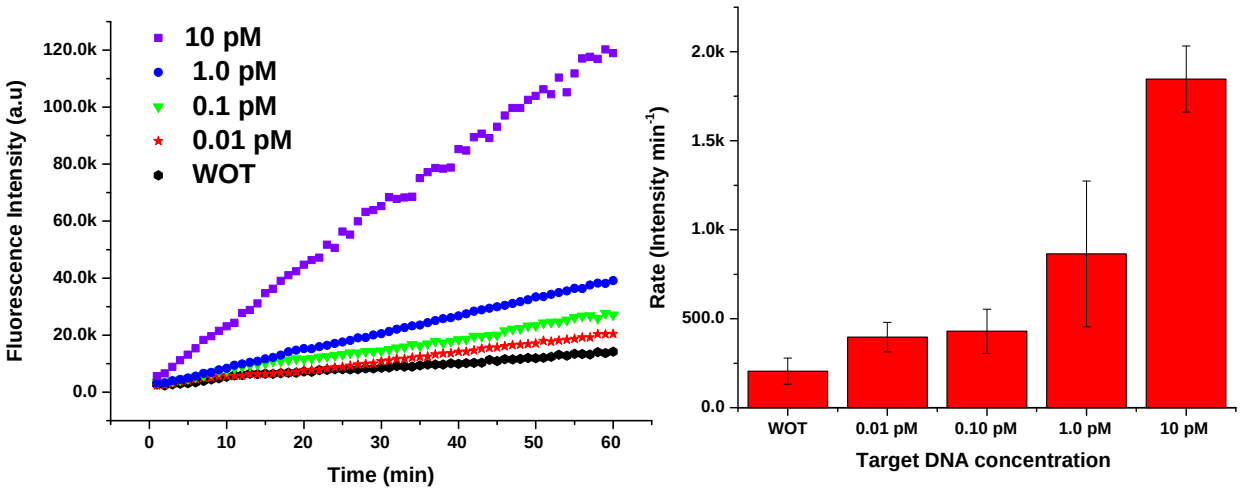

Figure S3. (**A**) Representative time-dependent fluorescence responses curves for detecting different concentrations (0.01 - 10 pM) of the full-match target-DNA (T1). (**B**) Typical fluorescence response rates for T1 detection (*n* =3).

Table S2. Comparison of the limit of detection (LOD) of some sensitive DNA assays and our MNP-enzyme sandwich assay using single enzyme amplification.

Sensing Method	LOD (pM)	Ref.
Photonic crystal hydrogel beads	0.66	2
Electrochemical detection based on bar-coded gold nanoparticles	~4	3
Magnetic particle-dye sandwich assay	100	4
Au particle-on-wire surface-enhanced Raman scattering (SERS)	10	5
Fluorescence based on Ag@poly(m-phenylenediamine) nanoparticles	250	6
Microcantilever array based nanomechanical sensing	10	7
Silver particle amplified surface enhanced Raman scattering	1-33	8
Graphene quenched fluorescence DNA nanoprobes	~100	9
Graphene-based high-efficiency surface-enhanced Raman scattering	10	10
Zn(II)-porphyrin/G-quadruplex complex with Exo III-assisted target recycle	200	11
MNP-enzyme probes detected *via* a personal glucose sensor	40	12
Electrochemical DNA sensing using a DNA tetrahedron structure	1	13
Gold nanoparticle amplified surface Plasmon resonance sensing	10	14
Electrochemical sensing *via* a DNA Super-sandwich Assembly	0.1	15
MNP-sandwich + ligation with single-enzyme amplification	~1	**This work**

Table S3. Comparison of the sensing performance of some ultrasensitive DNA assays, **LOD**: limit of detection, **DR**: detection dynamic range; **RCA**: rolling circle amplification.

Amplification and readout strategy	**LOD (aM)**	**DR (fM)**	**Ref**
Colorimetric readout using GNP + Ligase chain reaction	20	0.050-20	16
Electrochemical readout using CdTe QD + target recycling + RCA	11	$0.01\text{-}10^4$	17
Fluorescence readout using QD +Primer generation + RCA	50.9	$0.1\text{-}10^6$	18
Single particle fluorescence detection using QD entrapped liposome	1-2.5	?	19
Electrochemical readout using target recycling + signal amplifcation	10.9	$0.1\text{-}10^9$	20
Electrochemical sensing using graphene-supported ferric porphyrin	22	$0.1\text{-}10^4$	21
MNP-sandwich + ligation with poly-enzyme nanobead amplification	1.6	$0.001\text{-}10^3$	**This work**

References

(1) Susumu, K.; Mei, B. C.; Mattoussi, H. *Nat. Protoc.* **2009**, *4*, 424-436.

(2) Hu, J.; Zhao, X.-W.; Zhao, Y.-J.; Li, J.; Xu, W.-Y.; Wen, Z.-Y.; Xu, M.; Gu, Z.-Z. *J. Mater. Chem.* **2009**, *19*, 5730-5736.

(3) Zhang, D.; Huarng, M. C.; Alocilja, E. C. *Biosens. Bioelectron.* **2010**, *26*, 1736-1742.

(4) Liu, H.; Li, S.; Liu, L.; Tian, L.; He, N. *Biosens. Bioelectron.* **2010**, *26*, 1442-1448.

(5) Kang, T.; Yoo, S. M.; Yoon, I.; Lee, S. Y.; Kim, B. *Nano Lett.* **2010**, *10*, 1189-1193.

(6) Zhang, Y.; Wang, L.; Tian, J.; Li, H.; Luo, Y.; Sun, X. *Langmuir* **2011**, *27*, 2170-2175.

(7) Zhang, J.; Lang, H.-P.; Huber, F.; Bietsch, A.; Grange, W.; Certa, U.; McKendry, R.; Güntherodt, H.-J.; Hegner, M.; Gerber, C. *Nat. Nanotechnol.* **2006**, *1*, 214-220.

(8) Faulds, K.; McKenzie, F.; Smith, W. E.; Graham, D. *Angew. Chem., Int. Ed.* **2007**, *119*, 1861-1863.

(9) Zhang, M.; Yin, B.-C.; Tan, W.; Ye, B.-C. *Biosens. Bioelectron.* **2011**, *26*, 3260-3265.

(10) He, S.; Liu, K.-K.; Su, S.; Yan, J.; Mao, X.; Wang, D.; He, Y.; Li, L.-J.; Song, S.; Fan, C. *Anal. Chem.* **2012**, *84*, 4622-4627.

(11) Zhang, Z.; Sharon, E.; Freeman, R.; Liu, X.; Willner, I. *Anal. Chem.* **2012**, *84*, 4789-4797.

(12) Xiang, Y.; Lu, Y. *Anal. Chem.* **2012**, *84*, 1975-1980.

(13) Pei, H.; Lu, N.; Wen, Y.; Song, S.; Liu, Y.; Yan, H.; Fan, C. *Adv. Mater.* **2010**, *22*, 4754-4758.

(14) He, L.; Musick, M. D.; Nicewarner, S. R.; Salinas, F. G.; Benkovic, S. J.; Natan, M. J.; Keating, C. D. *J. Am. Chem. Soc.* **2000**, *122*, 9071-9077.

(15) Xia, F.; White, R. J.; Zuo, X.; Patterson, A.; Xiao, Y.; Kang, D.; Gong, X.; Plaxco, K. W.; Heeger, A. J. *J. Am. Chem. Soc.* **2010**, *132*, 14346-14348.

(16) Shen, W.; Deng, H.; Gao, Z. *J. Am. Chem. Soc*. **2012**, *134*, 14678-14681.

(17) Ji, H.; Yan, F.; Lei, J.; Ju, H. *Anal. Chem*. **2012**, *84*, 7166-7171.

(18) Zeng, Y.; Zhu, G.; Yang, X.; Cao, J.; Jing, Z.; Zhang, C. *Chem. Commun*. **2014**, *50*, 7160-7162.

(19) Zhou, J.; Wang, Q.; Zhang, C. *J. Am. Chem. Soc*. **2013**, *135*, 2056-2059.

(20) Zhao, Z.; Chen, S.; Wang, J.; Su, J.; Xu, J.; Mathur, S.; Fan, C.; Song, S. *Biosens. Bioelectron*. **2017**, *94*, 605-608.

(21) Wang, Q.; Lei, J.; Deng, S.; Zhang, L.; Ju, H. *Chem. Commun*. **2013**, *49*, 916-918.